Supporting Information for

Kinetics-Controlled Synthesis of Gold-Silver Nanosheets with Abundant in-Plane Cracking and Their Trimetallic Derivatives for Plasmon-Enhanced Catalysis

Yiqun Zheng,[a*] Gongguo Zhang,[a] Yanyun Ma,[b*] Yuhan Kong, Feng Liu,[c] and Maochang Liu[c]

[a] School of Chemistry, Chemical Engineering, and Materials, Jining University, Qufu, Shandong 273155, P. R. China

[b] Institute of Functional Nano & Soft Materials (FUNSOM), Jiangsu Key Laboratory for Carbon-Based Functional Materials & Devices, Soochow University, Suzhou, Jiangsu 215123, P. R. China

[d] International Research Center for Renewable Energy, National Key Laboratory of Multiphase Flow in Power Engineering, Xi'an Jiaotong University, Xi'an, Shaanxi 710049, China

[*]Corresponding author: Prof. Y. Zheng, whzyq@163.com; Prof. Y. Ma, mayanyun@suda.edu.cn

Number of Figure: 16

Number of Page: 17

Number of Table: 1

Table of Content

Figure S1. SEM image of the AuAg branched nanosheets.

Figure S2. Wide XPS spectrum of the AuAg branched nanosheets.

Figure S3. EDS spectrum of the AuAg branched nanosheets as shown in Figure 2.

Figure S4. TEM images showing the effect of injection rate of metal precursor on the AuAg product morphology.

Figure S5. TEM images showing the effect of reaction temperature on the AuAg product morphology.

Figure S6. TEM images showing the effect of Au/Ag molar ratio in precursor on the AuAg product morphology.

Figure S7. TEM images showing the effect of OTAC amount on the AuAg product morphology.

Figure S8. Wide XPS spectrum of the Au@PdAg nanosheets.

Figure S9. Wide XPS spectrum of the AuAgPt nanosheets.

Figure S10. EDS spectrum of the AuAgPd nanosheets as shown in Figure 4.

Figure S11. EDS spectrum of the AuAgPt nanosheets as shown in Figure 5.

Figure S12. XRD pattern of the AuAgPd nanosheets as shown in Figure 4.

Figure S13. XRD pattern of the AuAgPt nanosheets as shown in Figure 5.

Figure S14. Time-dependent UV-vis extinction spectra recorded under different irritation conditions using different metallic catalysts.

Figure S15. Plots showing c) the absorbance and d) $\ln(I_0/I_t)$ *versus* reaction time under different irritation conditions using different metallic catalysts.

Figure S16. Experimental results for the UV-vis light-assisted reduction of 4-NP with no catalyst present.

Table S1. XRD results and theoretical diffraction peak positions of the AuAgPd and AuAgPt nanosheets.

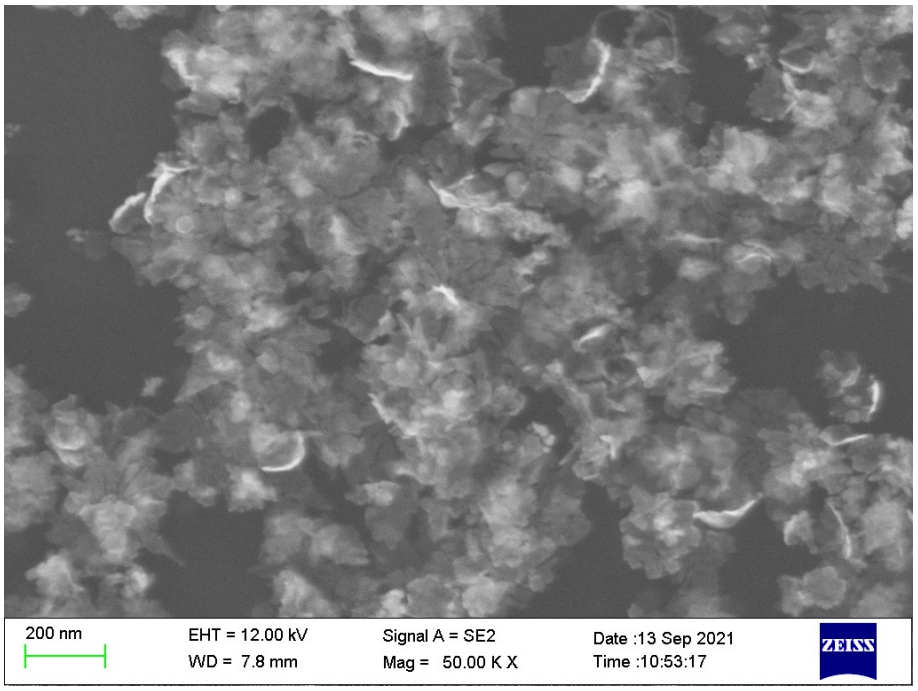

Figure S1. SEM image of AuAg branched nanosheets captured in another typical region.

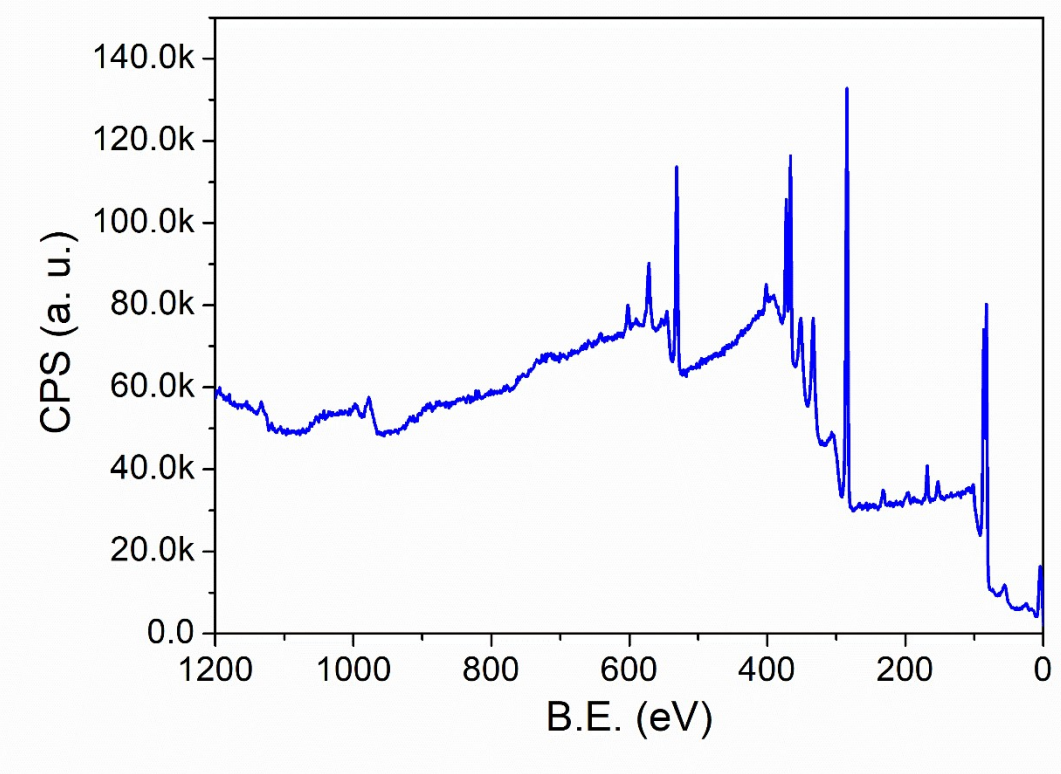

Figure S2. Wide XPS spectrum of the AuAg branched nanosheets.

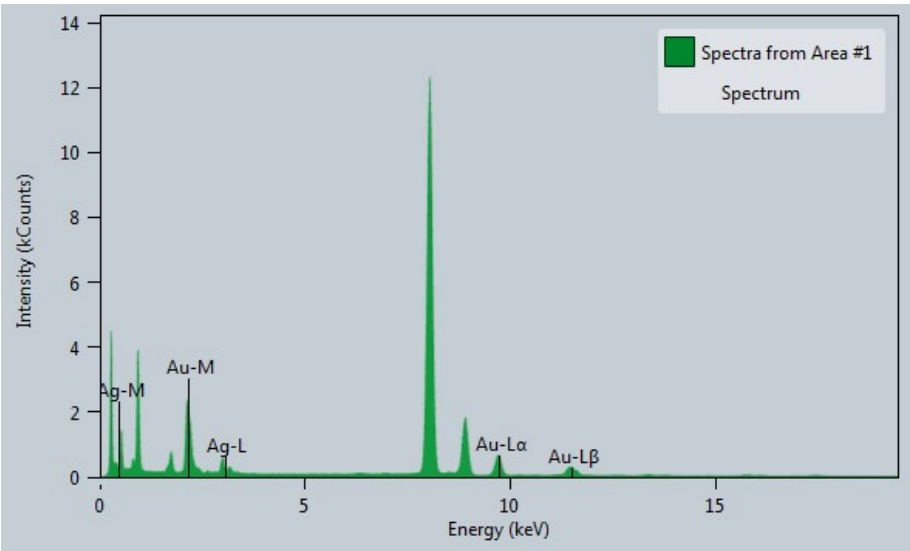

Figure S3. EDS spectrum of AuAg branched nanosheets as shown in Figure 2. The atomic molar ratio of Au:Ag was determined to be 67.9:32.1.

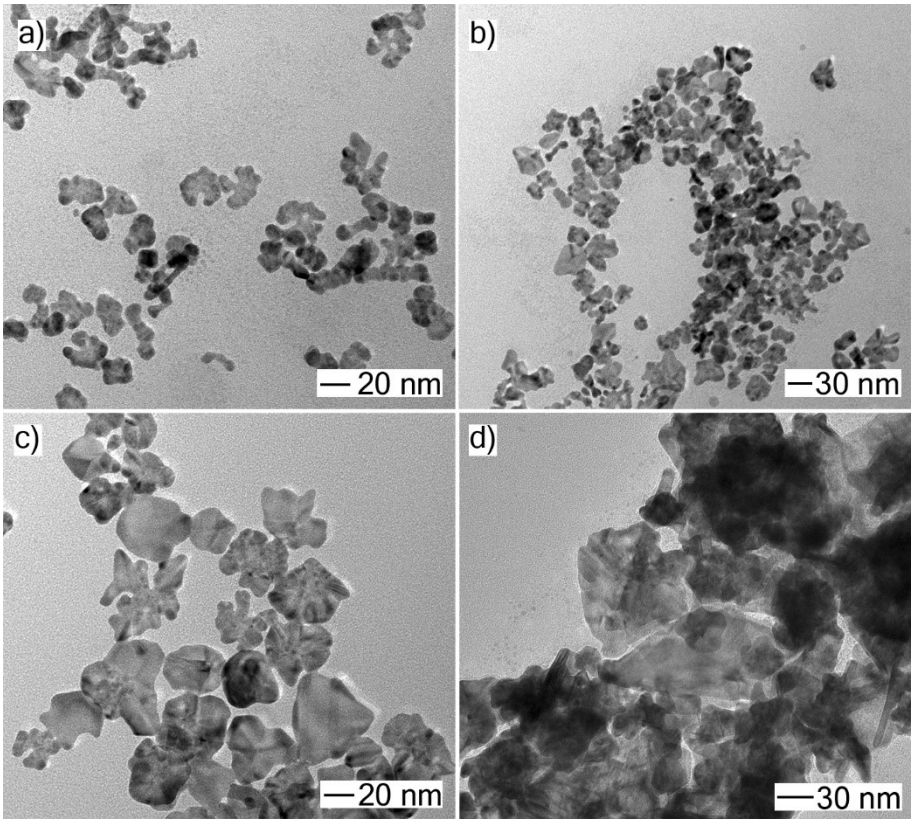

Figure S4. Effect of injection rate of metal precursor on AuAg product morphology. TEM images of products obtained *via* the P1 standard procedure, except that the Au-Ag precursor solution was dropwise added using a syringe pump at the injection rate of 4 mL/h, and the volume was controlled to a) 0.5 mL, b) 1 mL, c) 2 mL, and d) 4 mL, respectively.

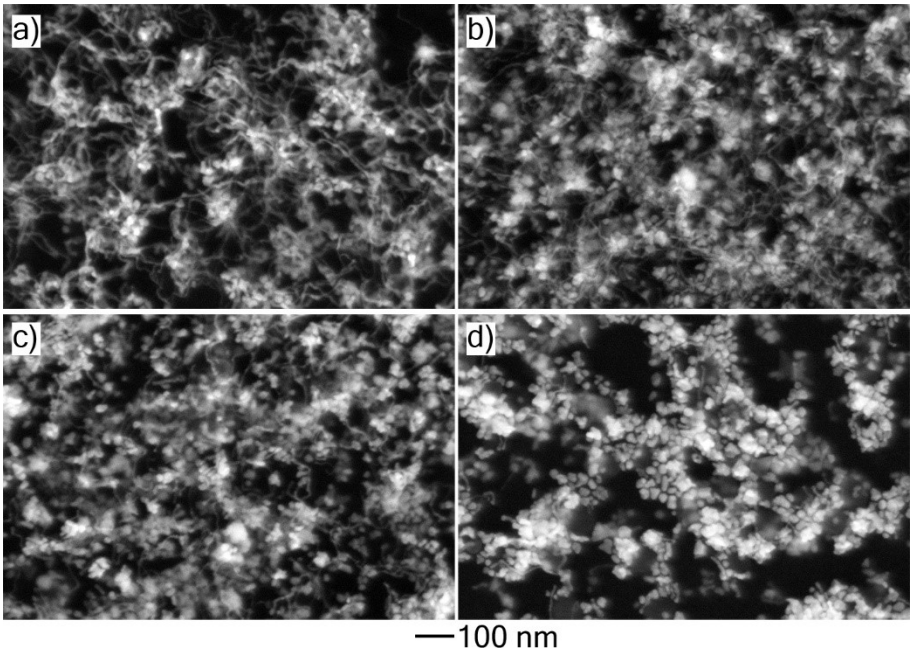

Figure S5. Effect of reaction temperature on AuAg product morphology. SEM images of products obtained *via* the standard procedure, except that the reaction temperature was set as 27 ^{o}C (room temperature) and the Au-Ag precursor solution was a) one-shot added and b-e) dropwise added using a syringe pump at the injection rate of c) 12 mL/h, d) 4 mL/h, and e) 2 mL/h, respectively.

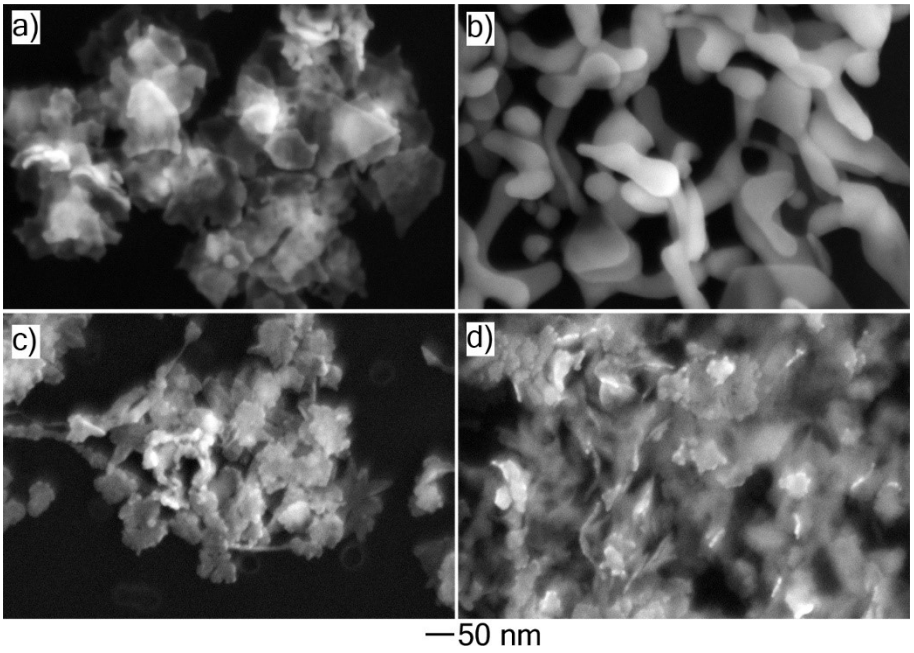

Figure S6. Effect of Au/Ag molar ratio in precursor on AuAg product morphology. SEM images of products obtained *via* the standard procedure, except that the injection rate was set at 12 mL/h and the concentration of precursor solution was varied to a) 0.5 mM $HAuCl_4$, b) 0.5 mM $AgNO_3$, c) 0.25 mM $HAuCl_4$+0.25 mM $AgNO_3$, d) 0.125 mM $HAuCl_4$+0.375 mM $AgNO_3$, respectively.

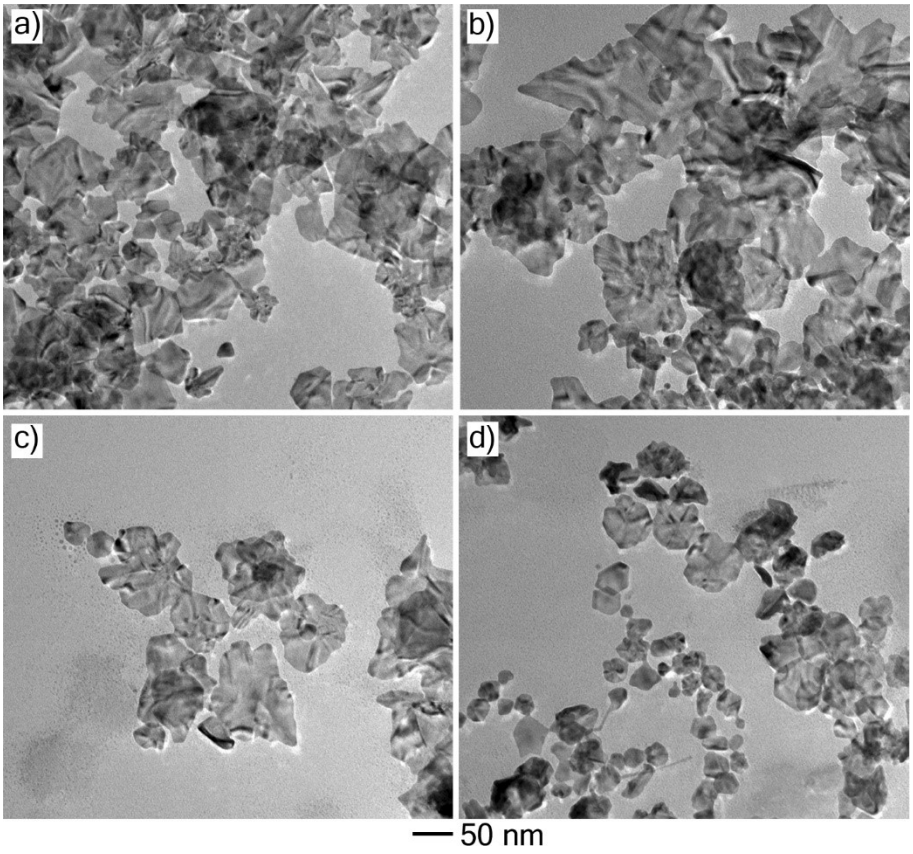

Figure S7. Effect of OTAC amount on AuAg product morphology. TEM images of AuAg products obtained *via* the standard procedure, except that the amount of OTAC was varied from 1000 μmol to a) 400, b) 200, c) 100, and d) 50 μmol, respectively.

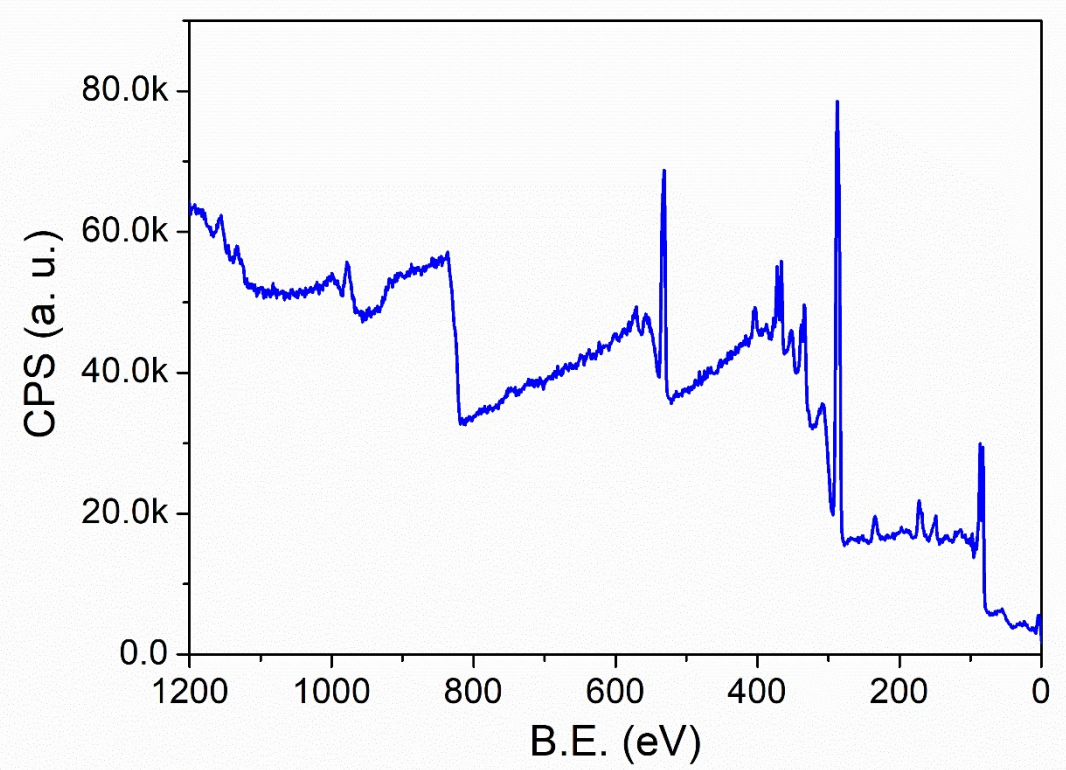

Figure S8. Wide XPS spectrum of the Au@PdAg nanosheets.

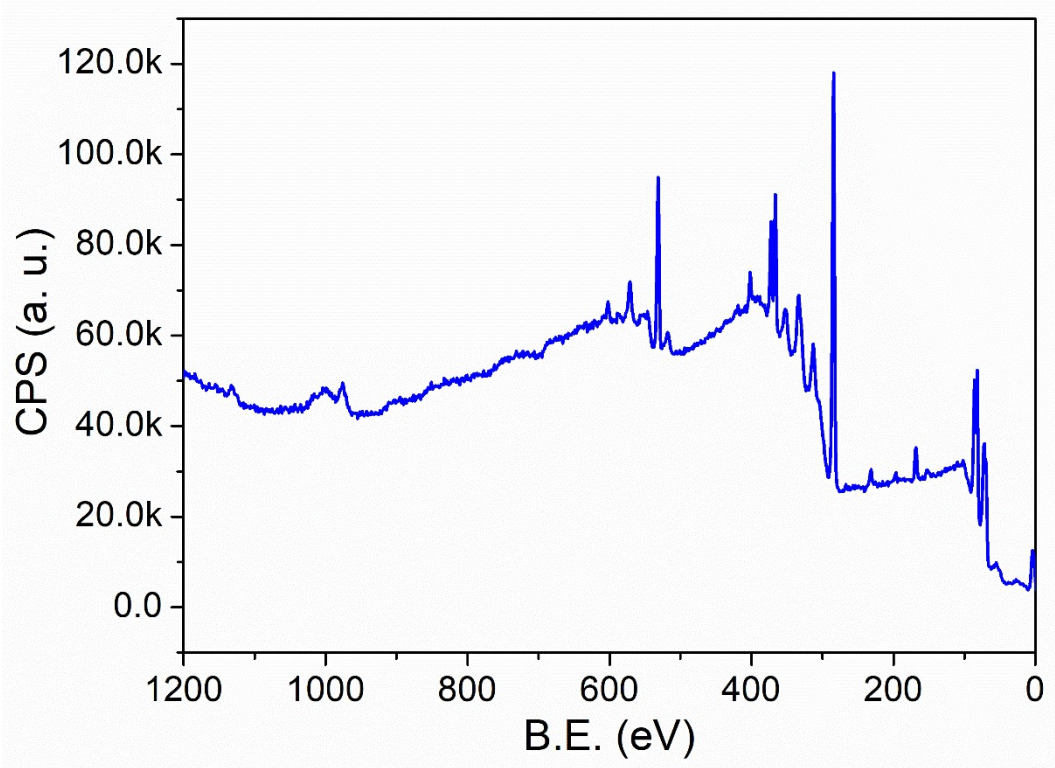

Figure S9. Wide XPS spectrum of the AuAgPt nanosheets.

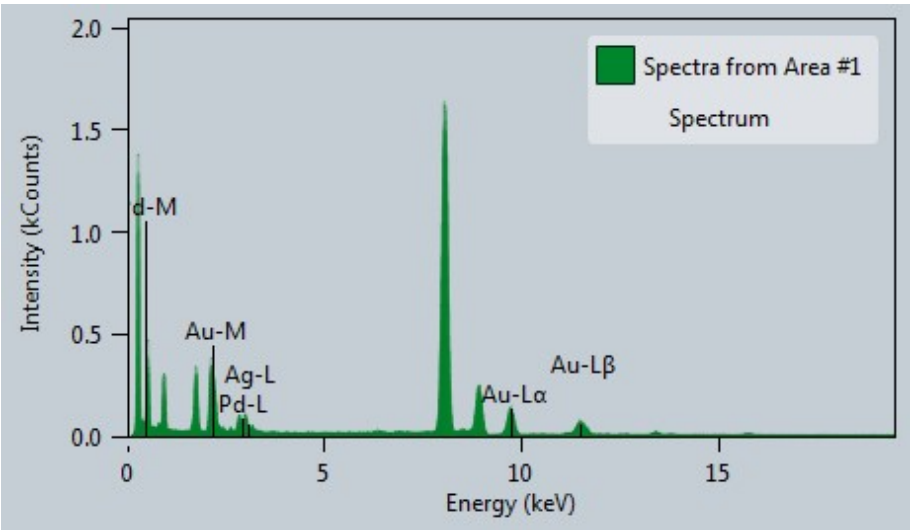

Figure S10. EDS spectrum of AuAgPd nanosheets as shown in Figure 4. The atomic molar ratio of Pd:Ag:Au was determined to be 22.7:14.6:62.7.

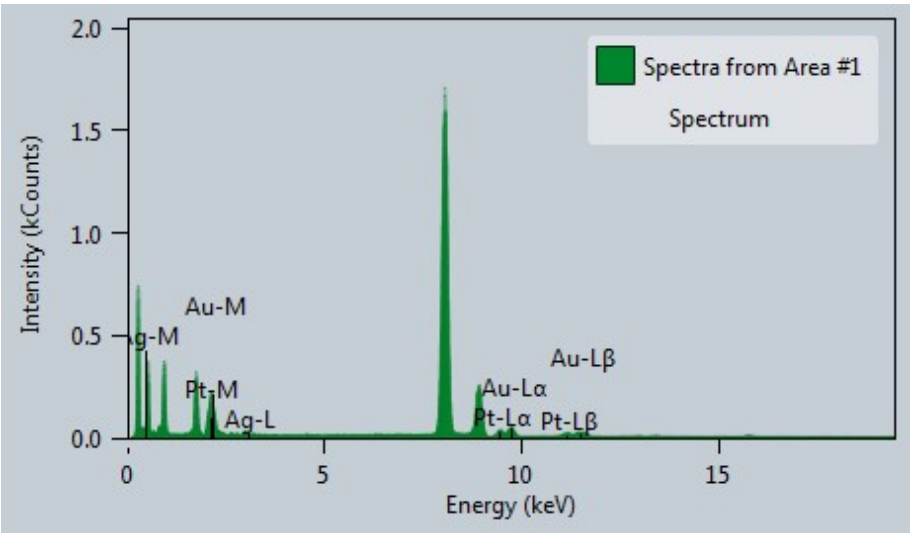

Figure S11. EDS spectrum of AuAgPt nanosheets as shown in Figure 5. The atomic molar ratio of Pt:Ag:Au was determined to be 33.2:14.1:52.7.

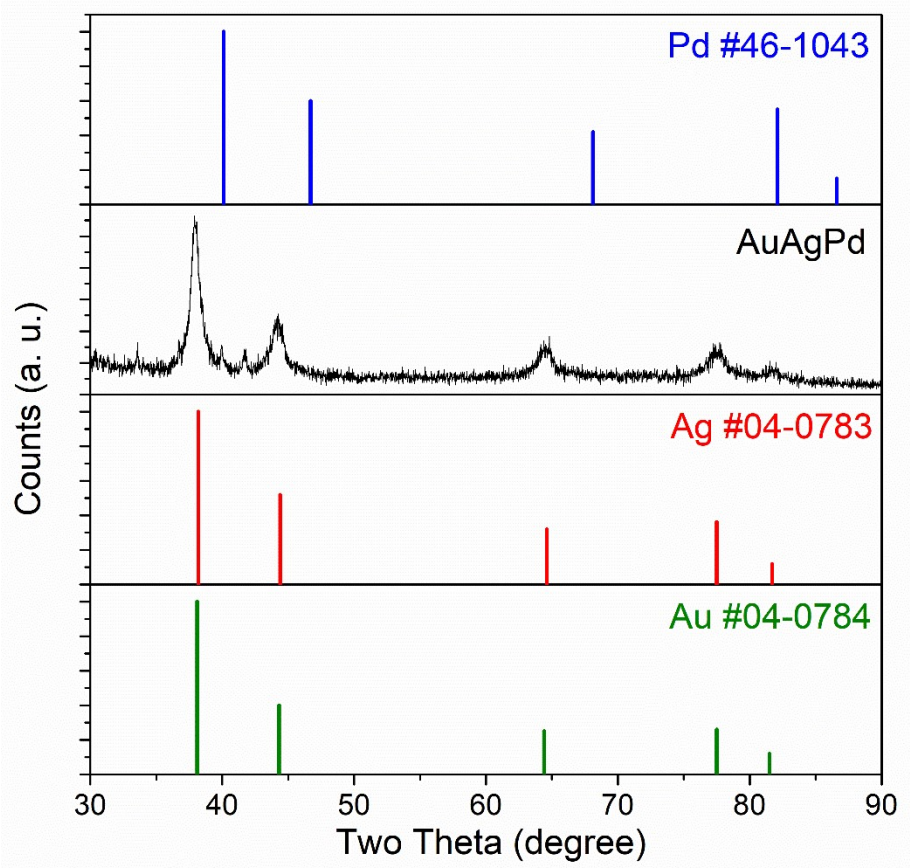

Figure S12. XRD pattern of AuAgPd nanosheets as shown in Figure 4. Data of *fcc*-Au (JCPDS No. 04-0784), *fcc*-Ag (JCPDS No. 04-0783), and *fcc*-Pd (JCPDS No. 46-1043) was provided for reference.

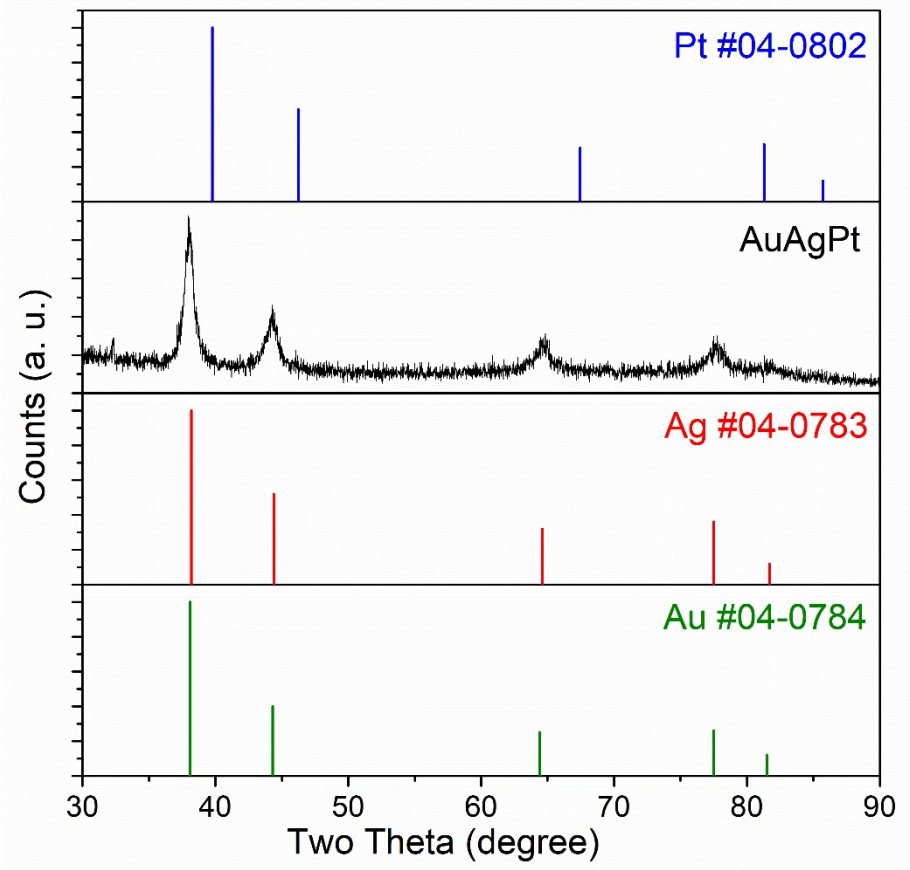

Figure S13. XRD pattern of AuAgPt nanosheets as shown in Figure 5. Data of *fcc*-Au (JCPDS No. 04-0784), *fcc*-Ag (JCPDS No. 04-0783), and *fcc*-Pt (JCPDS No. 04-0802) was provided for reference.

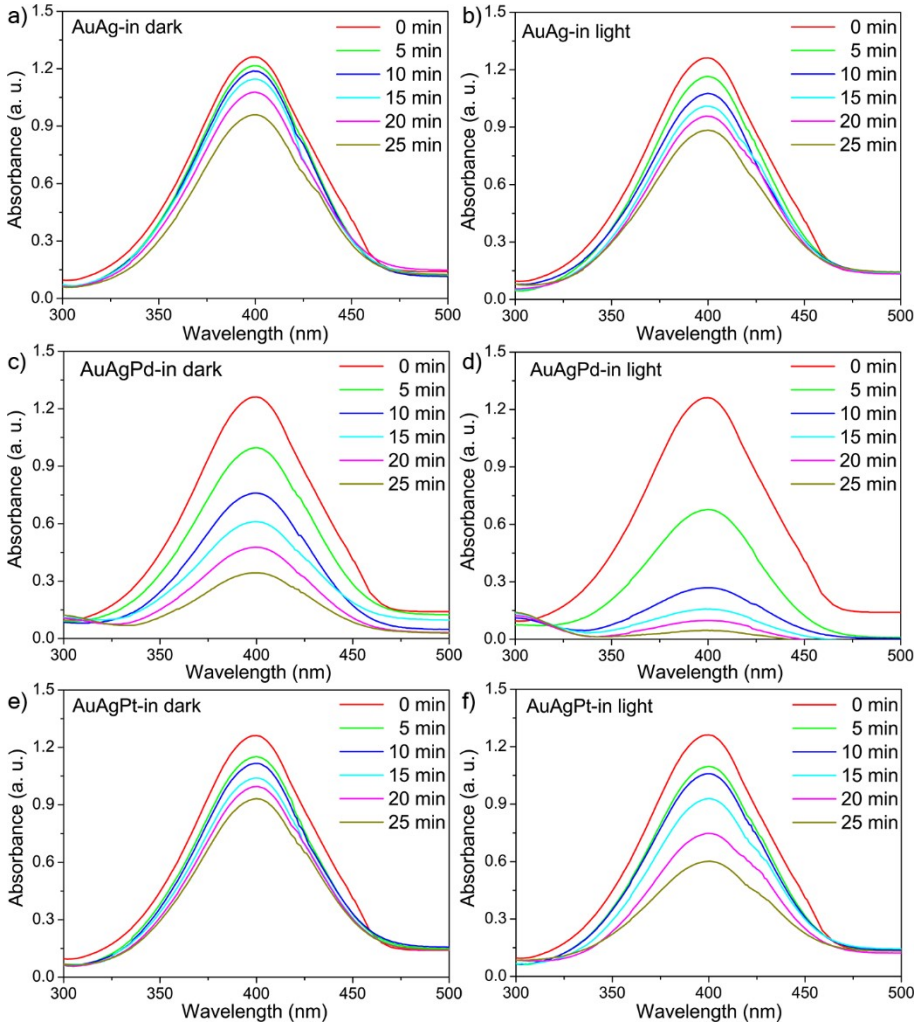

Figure S14. Time-dependent UV-vis extinction spectra recorded a, c, e) in light and b, d, f) in dark. Catalysts: a, b) AuAg; c, d) AuAgPd; e, f) AuAgPt. Condition: [$NaBH_4$] = 66.7 mM, [4-NP] = 0.07 mM, mass amount of catalyst = 40 μg, total volume = 15 mL.

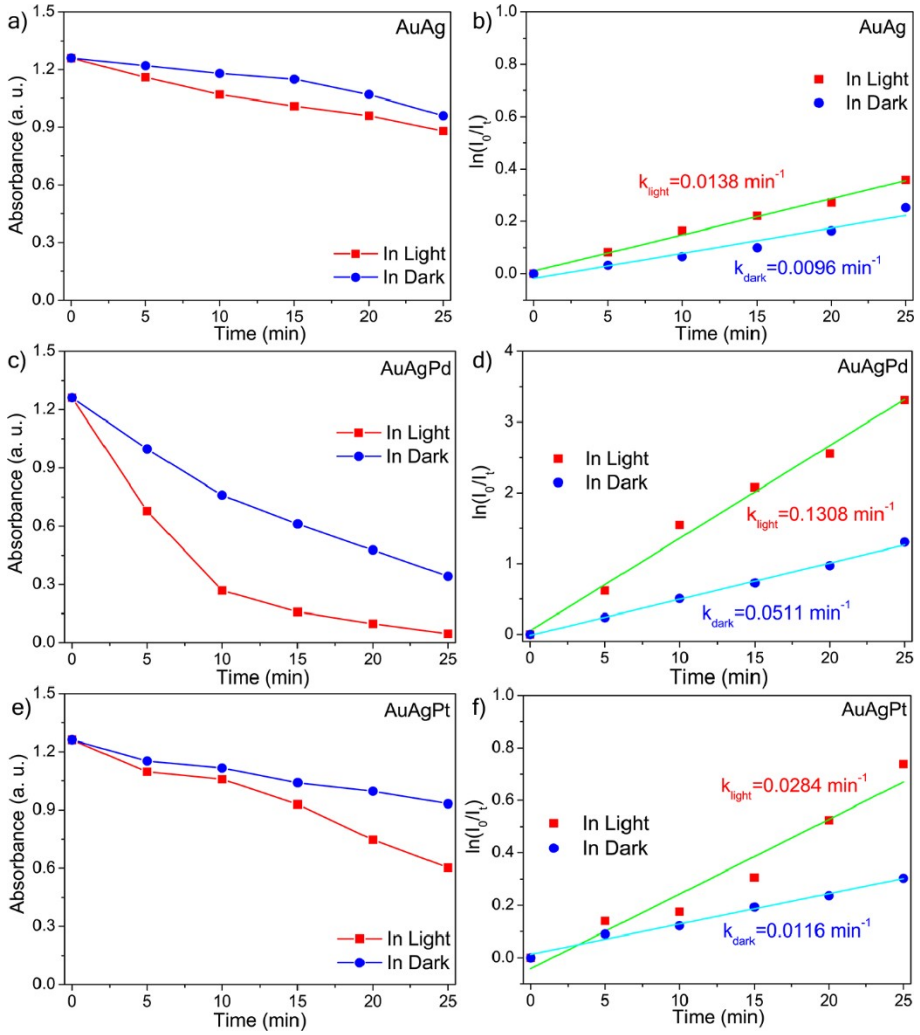

Figure S15. Plots showing c) the absorbance and d) $\ln(I_0/I_t)$ *versus* reaction time measured a, c, e) in light and b, d, f) in dark. Catalysts: a, b) AuAg; c, d) AuAgPd; e, f) AuAgPt. Condition: [$NaBH_4$] = 66.7 mM, [4-NP] = 0.07 mM, mass amount of catalyst = 40 μg, total volume = 15 mL.

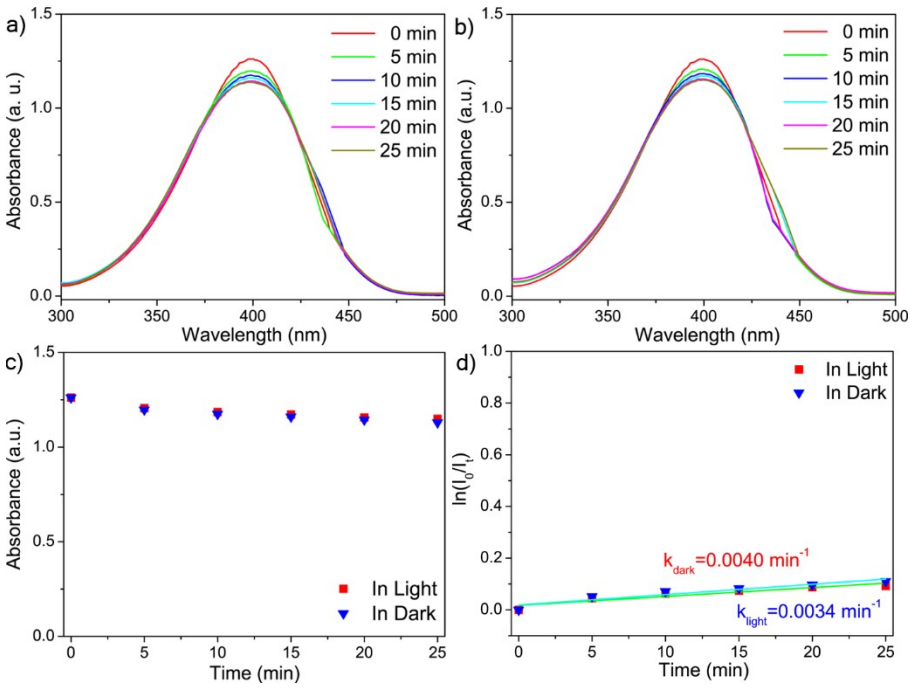

Figure S16. Experimental results for the UV-vis light-assisted reduction of 4-NP with no catalyst present: a, b) Time-dependent UV-vis extinction spectra recorded a) in dark and b) in light; c, d) Plots showing c) the absorbance and d) $\ln(I_0/I_t)$ *versus* reaction time. Condition: $[NaBH_4]$ = 66.7 mM, [4-NP] = 0.07 mM, total volume = 15 mL.

Table S1. XRD results and theoretical diffraction peak positions of as-prepared $Au_{62.7}Ag_{14.6}Pd_{22.7}$ and $Au_{52.7}Ag_{14.1}Pt_{33.2}$ nanosheets.

		Diffraction Peak Position (°)			
		(111)	(200)	(220)	(311)
$Au_{62.7}Ag_{14.6}Pd_{22.7}$	XRD	37.9	44.2	64.6	77.5
	Theoretical*	38.6	44.9	65.4	78.5
$Au_{52.7}Ag_{14.1}Pt_{33.2}$	XRD	38.0	44.3	64.7	77.6
	Theoretical*	38.7	45.0	65.5	78.8
Pd	JCPDS No. 46-1043	40.1	46.7	68.1	82.1
Pt	JCPDS No. 04-0802	39.8	46.2	67.5	81.3
Au	JCPDS No. 04-0784	38.2	44.4	64.6	77.5
Ag	JCPDS No. 04-0783	38.1	44.3	64.4	77.5

*The theoretical value was calculated using Vegard's Law.